We are IntechOpen, the world's leading publisher of Open Access books
Built by scientists, for scientists

6,900
Open access books available

185,000
International authors and editors

200M
Downloads

154
Countries delivered to

Our authors are among the

TOP 1%
most cited scientists

12.2%
Contributors from top 500 universities

BOOK CITATION INDEX
CLARIVATE ANALYTICS
INDEXED

WEB OF SCIENCE™

Selection of our books indexed in the Book Citation Index
in Web of Science™ Core Collection (BKCI)

Interested in publishing with us?
Contact book.department@intechopen.com

Numbers displayed above are based on latest data collected.
For more information visit www.intechopen.com

Achievable Capacity Limit of High Performance Nodes for Wireless Mesh Networks

Thomas Olwal, Moshe Masonta, Fisseha Mekuria and Kobus Roux

Additional information is available at the end of the chapter

1. Introduction

Research background: Next generation fixed wireless broadband networks have immensely been deployed as mesh networks in order to provide and extend access to the internet. These networks are characterised by the use of multiple orthogonal channels available within the industrial, scientific and medical (ISM) liscensed-free frequency bands. Nodes in the network have the ability to simultaneously communicate with many neighbours or stream different versions of the same data/information using multiple radio devices over orthogonal channels thereby improving effective "online" channel utilisation (Kodialam & Nandagopal, 2005). The ability to perform full duplex communication by individual multi-radio nodes without causing network interference has also been achieved through decentralized transmission power control schemes in (Olwal, 2010; Olwal et al., 2011). Allen et al. (2007) alluded that multiple radios that receive versions of the same transmission may together correctly recover a frame that would otherwise be lost based on multipath fading, even when any given individual radio cannot. Many such networks emerging from standards such as IEEE 802.11 a/b/g/n and 802.16 are already in use, ranging from prototype testbeds (Eriksson et al., 2006) to complete solutions (Mesh Dynamics, 2010).

The increasing question is how the theoretical capacity of such static multi-radio multi-channel (MRMC) network scales with the node density, irregularity of the terrain and the presence of tree foliage (Intini, 2000). In their seminal work, Gupta and Kumar (2000) determined the capacity of single radio single channel networks. Their findings have been later extended to derive the capacity bounds of the MRMC configurations of a network scope by Kyasanur and Vaidya (2005). In addition, the link throughput performance parameters in IEEE 802.11 networks have also been discussed in Berthilson & Pascual (2007). However, the considered MRMC network architecture has so far been presented with a number of impractical assumptions. The first assumption asserts that the location of nodes and traffic patterns can be controlled in arbitrary networks. The second assumption claims that channel fading

can be excluded in the capacity analysis such that each frequency channel can support a fixed data rate. Lastly, nodes are randomly located on the surface of a torus of unit area to avoid technicalities arising out of edge effects. However, in realistic networks, location of nodes is determined by the irregularity of the terrain, the presence of tree foliage (Tse & Viswanath, 2005), and users' needs and their locations (Makitla et al., 2010). Moreover, typical rural based wireless networks can be described by (i) long single hop links, (ii) limited and unreliable energy sources, and (iii) clustered distribution of Internet users (Ishamel et al., 2008).

In order to address some of these issues and obtain high network throughput performance, high performance nodes (HPNs)™ for community-owned wireless mesh networks, have been implemented in most parts of rural South Africa (Kobus, et al., 2009). The innovation as shown in Figure 1, has been developed by the CSIR Meraka Institute and it provides high network throughput (capacity). The HPN™ is an IEEE 802.11 based multi-interface node made up of three interfaces or radio devices and controlled by an embedded microcontroller technology (Makitla et al., 2010). To ensure high speed performance, the innovation has the first radio interface card attached to a 5 GHz directional antenna for backhaul mesh routing, the second interface card is connected to a 5 GHz omni-directional antenna for backhaul mesh connectivity and access. The third radio interface card is attached to a 2.4 GHz omni-directional antenna for mesh client access network. As shown in Figure 2, the HPN block diagram has a weather proof Unshielded Twisted Pair (UTP) connector at the bottom of the node that provides Power-Over-Ethernet (PoE) and Ethernet connectivity to the HPN. To attach the HPN to a pole or a suitable structure, a mounting bracket is fixed at the back of the router (See Makitla et al., 2010) for other operational details. The HPNs are often installed on roof tops, street poles and buildings of villages, local schools, clinics, museums and agricultural farmlands.

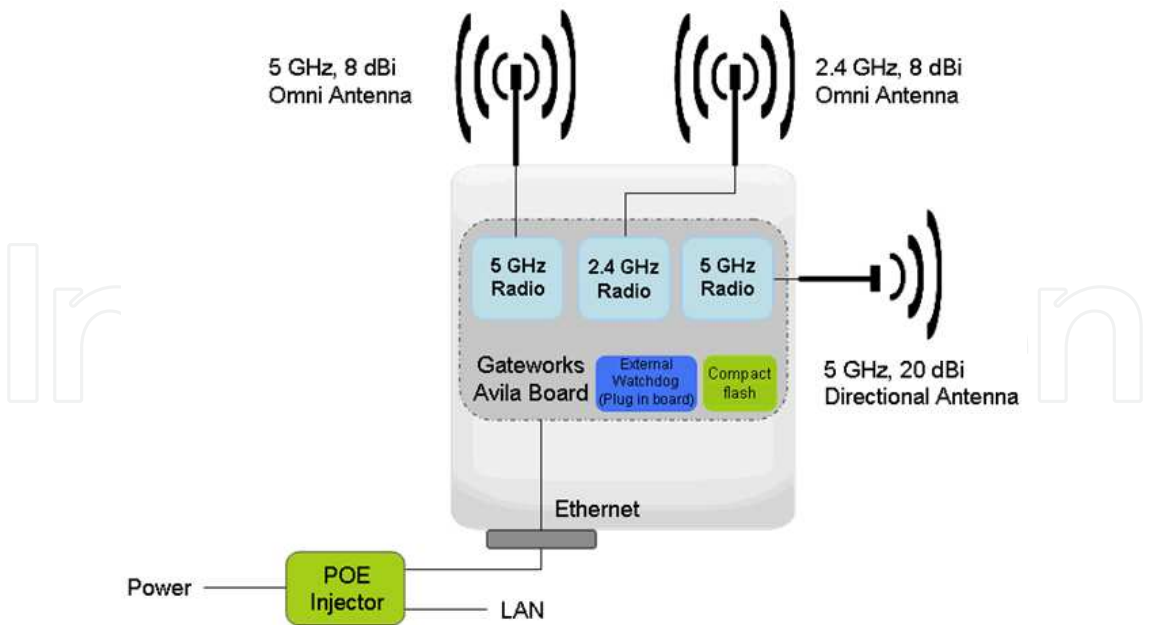**Figure 1.** High performance node (HPN)™ (Makitla et al., 2010)

Figure 2. Block diagram of HPN™ (Makitla et al., 2010)

In this study, we shall concentrate on the backhaul terminal connectivity of the HPNs. The backhaul terminal connectivity offers aggregated traffic volumes of all flows within the network. The traffic flows traverse long links between any two HPNs and are faced with severe climatic conditions. Thus, evaluating the capacity limits of such links provides useful inputs toward optimal design of the cross-layer protocols. Figure 3 illustrates the broadband for all (BB4all™) architecture of a single wireless link based on two HPNs (that is, Node A and Node B) with end to end (E2E) Ethernet cable.
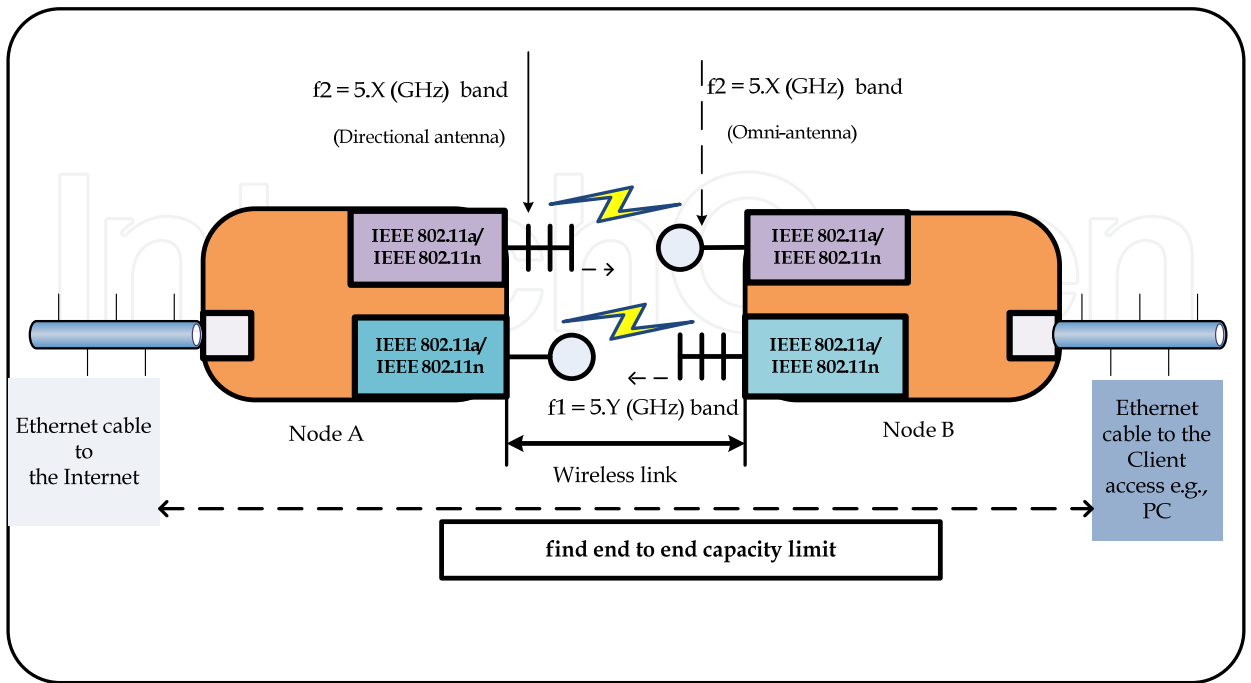

Figure 3. Single link architecture of HPNs

Research problem or questions: The main problem constitutes the need to increase capacity of community owned existing wireless broadband networks so that network users can scale without losing any connectivity and multimedia services can be provided in remote and rural areas (Mekuria et al., 2012). This problem is further subdivided into a number of research questions. Firstly, what is the achievable capacity limit of the HPNs based on IEEE 802.11a air interface under multipath fading channels (Tse & Viswanath, 2005)? Secondly, what is the achievable capacity limit of the HPNs based on IEEE 802.11n air interface under multi-input multi-output (MIMO) fading channels? Thirdly, what is the achievable end-to-end (E2E) capacity limit in HPNs in community mesh networks under: regular, irregular, and clustered node placements? The study assumes that there is no frequent channel switching even though the number of channels may be greater than the number of radios per node (Olwal, 2010). This implies that, non overlapping channels are assigned statically to available radio devices over a transmission period. Statically assigned channel over a given interval is a reasonable consideration since there is high probability that traffic volumes in rural areas are low compared to urban areas most of the times.

Research objectives: In order to investigate the capacity performance of the HPNs, the first aim of this chapter is to characterize the impact of multipath and MIMO fading channels on achievable theoretical capacity limits of single links IEEE 802.11a and IEEE 802.11n based standards. The second aim is to derive the impact of number of interfaces and channels per each HPN on the E2E capacity limits of BB4all™ mesh networks. This objective is achieved by considering a varying node density over a fixed deployment area, and the rate of a single wireless link that depends on the physical communication barriers.

Methodology: In order to achieve these objectives, firstly, the per link capacity limit under frequency selective channel is developed using conventional approaches in literature. The analytical capacity results of the BB4all™ architecture are numerically compared to IEEE 802.11a standard data sheet in order to understand the performance gain of HPNs. Secondly, the per link capacity limit for MIMO fading channels is developed and the results are numerically compared to IEEE 802.11n standard data sheet in order to show case the benefits of HPNs. Thirdly, given a typical rural community network with a pre-defined deployment area having varying node density, the impact of interfaces and channels per node on the capacity of BB4all™ mesh architecture is derived. The capacity limits of regular, irregular and cluster network topologies are obtained and compared with results from Kyasanur and Vaidya (2005) for arbitrary networks.

Research results: Analytical results indicate that the multipath fading channels and MIMO channels can be exploited to improve channel diversity in community mesh networks. Diversity improves capacity of wireless links over multiple paths and through multiple frequency channels. For regular, irregular and clustered node placements, the following analytical results were obtained for *the upper bound end-to-end capacity limit*, respectively,

$$O\left(nR\sqrt{\frac{mc}{\delta}} \right), O\left(Rn\sqrt{\frac{mc}{\delta p}} \right), \text{and } O\left(R\sqrt{\frac{nmc}{1}\left(\frac{n_1}{\delta_1} + \frac{n_2}{\delta_2} \right)} \right).$$

Here, R is the single link rate in bits/s computed by taking into account multipath effects and innovative HPNs built-in structure, n is the number of HPNs, m is the number of radio interface cards per each HPN, c is the number of frequency channels that do not cause interference in duplex communication, $0 < p < 1$ is the irregularity rate (probability) of HPN placement, and δ is the HPN distribution density that is varied over a fixed deployment area.

The rest of the chapter is organised as follows. Section 2 provides a description of a typical rural community mesh network in which the BB4all™ architecture proposal can be applied. In Section 3, issues of theoretical capacity limits for single links are discussed. Section 4 analyses upper bound capacity limits for mesh networks in real deployments. Section 5 furnishes the numerical capacity limit of a selected real network in a given rural area size. The chapter is concluded with highlights of the main contribution of this study and future research and development (R&D) perspectives.

## 2. Rural community mesh network: A case of Peebles valley mesh in South Africa

Peebles valley mesh (PVM) is a typical rural community mesh network that is funded by the International Development Research Centre (IDRC) and is deployed in Mpumalanga province in South Africa (Johnson, 2007). The conventional PVM network, consists of nine (9) single radio nodes, and covers an area of about 15 square kilometres in Masoyi tribal land. The Masoyi tribal land is located at the North East of White River along the road to the Kruger National Park in South Africa. The land is hilly with some large granite outcrops and it has a valley that stretches from the AIDS care training and support (ACTS) clinic and divides the wealthy commercial farms from the poorer Masoyi tribal area. The Masoyi community is underserviced with lack of tarmac roads and most houses are lacking running water. However, there is unreliable electricity present in the Masoyi area. The power outages occur on average one outage in seven days and might even last up to a full day (i.e., 24 hours). Albeit the government subsidizes the cost of electricity, a large population cannot afford electricity fees due to the low economic levels of the area. ACTS clinic (a non-governmental organization sponsored clinic) provides medical services to AIDS patients, counseling, testing and Anti-retroviral (ARV) treatment (Johnson & Roux, 2008).

Figure 4 demonstrates architecture of the PVM network when HPNs are deployed. In this figure, the clinic connects to surrounding schools, homes, farms and other clinic infrastructure through a mesh network. The network is seen as community asset with some of the equipment at key nodes are actually belonging to the community. In this area mesh connectivity offers:

- Scalable connectivity to the hilly terrain, over multiple hops based long distances and through non line of sight (NLOS).
- Auto-configurable traffic routing mechanisms with minimal human interventions. This feature ensures network sustainability in an area with apparent low skilled technical-personnel who cannot regularly maintain the network.

- Auto-organizable connectivity against severe climatic conditions that commonly cause links, nodes, and network failures in the area.

(Source: *http://wirelessafrica.meraka.org.za/*)
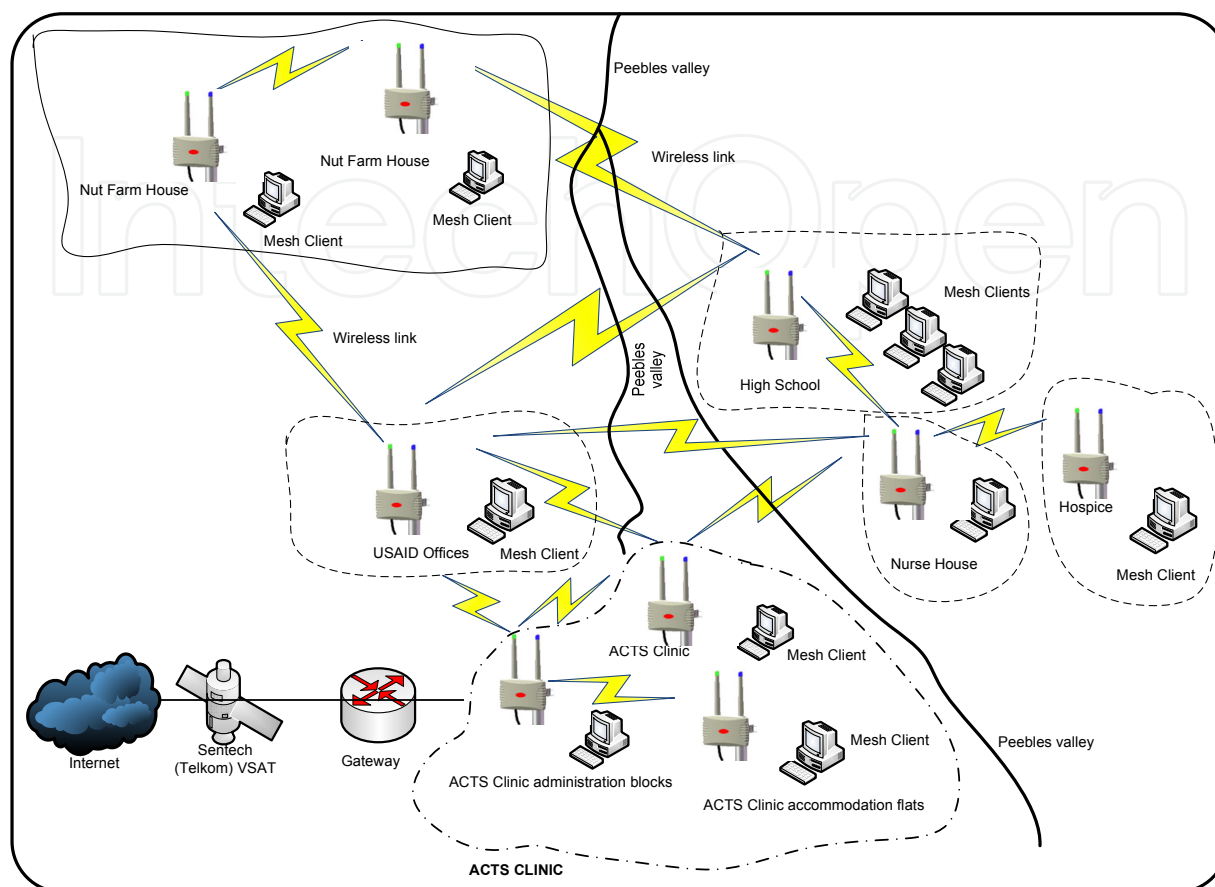
Figure 4. Mesh network architecture at Peebles valley in South Africa

Traditionally, the PVM is endowed with VSAT link that provides the network at the clinic with 2 Gbits per month at a download rate of 256 kbps and an upload rate of 64 kbps (Johnson & Roux 2008). The clinic provides 400 Mbps per month available to the single radio mesh network. The single radio mesh has nine users (mesh routers) so that each user (mesh router) receives about 44.4 Mbps per month on average. This traffic bandwidth drops downstream the network from the satellite gateway to the terminal users. This is due to lack of single radio network resiliency against effects of wireless multipath. However, in this document we believe that the design of the HPNs making the BB4all™ architecture can be a suitable candidate for improved capacity in multipath environment (BelAir Networks, 2006). As a result high data rates as the network scales away from the satellite gateway can be realized in the PVM deployment. The HPNs utilize the multiplicity of the low cost radio devices and non-overlapping channels to improve capacity delivered across the network.

Thus, the BB4all™ architecture constitutes a gateway connected to the internet via Sentech VSAT to the Peebles valley or ACTS clinic. Within the ACTS clinic there can be mesh

servers, personal computers as the mesh clients and HPNs may be installed to serve as wireless routers that link ACTS clinic accommodation flats to USAID offices about 1 Km away. The HPN link can connect Legogote Hospice and USAID premises about 3.35 Km over the valley via the Nurse house. The link over the valley between the USAID and Sakhile high school is about 2.4 Km. The link from Sakhile high school to the Legogote Hospice is about 4.6 Km, and the distance from high school to the farmers' houses is about 5.55 Km over the Peebles valley. It is also anticipated that the mesh network will expand to public clinics and schools that are farther way even up to 25 Km from the ACTS clinic center in the near future.

In conclusion the rural PVM project has triggered further insights for newer research, development and innovation. The terrain irregularity, the long distances, the tree foliage coupled with the need for high capacity Internet provision in rural communities are the key drivers for the BB4all™ connectivity solution. It is also noted that clear understanding of classical physical channel models combined with innovative ICT products is expected to promote sustainable internet services to billions including previously disadvantaged subscribers (Mekuria et al., 2012).

3. Achievable capacity limit for a single link with multipath fading

In order to realize long distance coverages by single links with multipath effects in wireless mesh networks in rural areas, the IEEE 802.11a and IEEE 802.11n standards commodity devices can be used. This is because these devices are off-the-shelves, operate in multiple ISM channel bands and are affordable to the rural communities (Kyansanur & Vaidya, 2004). That is to say that only fewer radio interface cards at each node are needed than the number of non-overlapping frequency channels freely available. Kyasanur and Vaidya emphasized how expensive it could be to equip a node with one interface card for each frequency channel. The IEEE 802.11a standard, for example, offers 24+ non-overlapping channels and configuring a commensurate number of radio interface cards on each node might be unnecessary costly. As a result, many IEEE 802.11 interface cards can be switched from one channel to another, albeit at the cost of a switching delay. Moreover, the advantage of eliminating frame losses due to path-dependent (e.g., multipath fading effects), location-dependent (e.g., noise effects), and statistically independence between different receiving radios can be achieved by using multi-radio diversity principle (Miu, Balakrishnan & Koksal, 2007). The idea is that even when each individual reception of a data frame is erroneous, it might still be possible to combine the different versions to recover the correct version of the frame. In this study, the question to be addressed is that what is the capacity expression for single links with multipath effects in a rural based wireless mesh network. It is understood that most of previous studies solve capacity problem with simple channel models that may not reflect the true wireless channel conditions (Gupta & Kumar, 2000).

3.1. IEEE 802.11a air interface

The standard IEEE 802.11a specifies an over-the-air interface between two wireless routers or between a wireless client and a router. It provides up to 54 Mbps in the 5 GHz frequency band and uses an orthogonal frequency division multiplexing (OFDM) encoding scheme.

This implies that a frequency selective channel is the most suitable approach to model the IEEE 802.11a air interface (Tse & Viswanath, 2005). This is because a frequency selective channel perfectly captures effects of multipath on signal propagation (i.e., due to terrain irregularity and tree foliage). The OFDM scheme is basically the preferred method to the frequency hopping spread spectrum (FHSS) or direct sequence spread spectrum (DSSS) schemes due to its robust performance over multipath. In this context, the IEEE 802.11a radio interface cards (Intini, 2000) make use of OFDM to provide high capacity over parallel wireless channels. In their definition, Tse and Viswanath (2005) states that a parallel channel is a channel which consists of a set of non-interfering sub-channels, each of which is corrupted by independent additive white Gaussian noise (AWGN).

To obtain the capacity over single link wireless medium, we assume each mth sub-channel of a parrallel channel is allocated a waterfilling power p_m such that the average power constraint P is still met on each input OFDM symbol to the multipath channel. Also consider that the AWGN power level to a parallel channel is N_0 and the co-channel interference caused by neighbouring transmissions is denoted as I. These parameters may be held constant in practice considering that most rural network applications are characterized by constant and low interference levels (Ismael et al., 2008). Then, the maximum capacity per every OFDM symbol of a reliable communication over M_c parallel streams or subcarriers is given by:

$$R_{M_c} = \sum_{m=0}^{M_c-1} \log_2\left(1 + \frac{p_m |\tilde{h}_m|^2}{(N_0 + I)}\right), \text{ bits / OFDM symbol,} \tag{1}$$

whereby the achievable capacity per link in bits/s/Hz for each parallel stream is written as

$$R_{multipath} = R_{M_c} / M_c, \text{ bits / s / Hz.} \tag{2}$$

Resulting from (2), the link capacity of a propagating OFDM signal over a wireless multipath channel is expanded in terms of the exponential function of the channel gain:

$$R_{OFDM/multipath} = \frac{1}{M_c}\sum_{m=1}^{M_c} \log_2\left(1 + \frac{p_m}{(N_0 + I)} \times |\tilde{h}_m|^2\right), \text{ bits / s / Hz}$$

$$R_{OFDM/multipath} = \frac{1}{M_c}\sum_{m=1}^{M_c} \log_2\left(1 + \frac{p_m}{(N_0 + I)} \times \left|\sum_{l=1}^{L} h_l \exp\left(-\frac{j2\pi lm}{M_c}\right)\right|^2\right), \text{ bits / s / Hz} \tag{3}$$

The achievable capacity of IEEE 802.11a air interface in terms of antenna gains (each antenna system for each radio interface), the range distances, the path loss exponent, the path multiplicity, and over the total bandwidth, W is defined as:

$$R_{OFDM/multipath} \approx W\log_2\left(1 + \frac{P}{(N_0 + I)} \times L^2 \times \frac{K_{antenna} d_0^\alpha}{d^\alpha}\right), \text{ bits / s.} \tag{4}$$

From (4), P is the maximum power allowed per sub-carrier, L is the number of paths associated to each sub-carrier and α is the path loss exponent. We denote $\mathrm{K}_{antenna}$ as the combined antenna gain which is simply the product of the transmitter and the receiver antenna gains, d_0 is the reference distance (Abhayawardhana et al., 2007). The combined antenna gain is thus, expressed as:

$$\mathrm{K}_{antenna} = \mathrm{K}_{antennaTxT} \times \mathrm{K}_{antennaRxV} \tag{5}$$

Inserting the result in (5) into the expression in (4) reveals that the higher the combined antenna gain, the higher the achievable link capacity. The improved antenna gain is the main attractive feature that the HPN based BB4all™ architecture offers to the conventional standards (Makitla, Makan & Roux, 2010). From (3), to view effects of frequency $f = nW/M_c$ on the time invariant wireless channel $\tilde{h}_m$, the known Fourier Transform (Bracewell, 1986) can be invoked:

$$\tilde{h}_m = \sum_{l=0}^{L-1} h_l \exp\left(-\frac{j2\pi lm}{M_c}\right) \Leftrightarrow H(f) = \sum_{l=0}^{L-1} h_l \exp\left(-\frac{j2\pi lf}{W}\right), \tag{6}$$

where $f \in [0, W]$. It should be deduced from the exponential relation that lowering f increases the gain in (6) that in turn increases the capacity limit in (4). Suppose we let that between any two mesh nodes directly connected there exists a clear line of sight (LOS) as it is the usual case in a mesh network. Then, the following multipath channel simplification can be made:

$$\left|\tilde{h}_m\right| = \left|\sum_{l=1}^{L} h_l \exp\left(-\frac{j2\pi lm}{M_c}\right)\right| = \sum_{l=1}^{L} |h_l|. \tag{7}$$

Based on these simplication, it is worthwhile noting that effects of multipath often produce inter-symbol interference (ISI), signal attentuation and multipath echoes. This leads to significant capacity drops. Fortunately, the OFDM communication exploits these channel diversity to improve capacity. Therefore, joint OFDM and HPN structural configurations can be utilised for capacity improvement in rural based networks.

3.2. IEEE 802.11n air interface

In the case of IEEE 802.11n air interface, the model of the wireless channel is characterized by antenna arrays with LOS and reflected paths as shown in Figure 5. The difference with IEEE 802.11a air interface is that multiple antennas are required at both transceivers when constructing the IEEE 802.11n HPNs. In this way, the LOS and reflected paths present wireless channel diversity that multi-input multi-output (MIMO) techniques need to exploit for channel capacity enhancement. In particular, if the direct path is denoted as *path 1* and the reflected path is denoted as *path 2*, then the channel **H** is given by the principle of superposition (Franceschetti et al, 2009):

$$\mathbf{H} = a_1^b \mathbf{e_r}\left(\Omega_{r1}\right)\mathbf{e_t}\left(\Omega_{t1}\right)^* + a_2^b \mathbf{e}_r\left(\Omega_{r2}\right)\mathbf{e_r}\left(\Omega_{t2}\right)^*, \text{for } i = 1, 2 \qquad (8)$$

with, $a_i^b = a_i\sqrt{n_t n_r}\exp\left(-\dfrac{j2\pi d^{(i)}}{\lambda_c}\right)$, where n_t is the number of transmit antennas, n_r is the number of receive antennas and λ_c is the wavelength of the pass-band transmitted signal. The distance between the transmit antenna 1 and recieve antenna 1 along path i is denoted by $d^{(i)}$. Figure 5 illustrates transmit and receive antenna arrays that is seperated by a concatenation of two channel $\mathbf{H}'$ and $\mathbf{H}''$ with virtual relays A and B. According to expression (8) and Figure 5, the unit spatial signature in the directional cosine Ω (i.e., $\Omega = \cos\phi$) is defined as follows:

$$\mathbf{e}_r(.) = \frac{1}{\sqrt{n_r}}\begin{pmatrix}1\\ \exp\left(-j2\pi\Delta_r\Omega\right)\\ \exp\left(-j2\pi 2\Delta_r\Omega\right)\\ .\\ .\\ .\\ \exp\left(-j2\pi\left(n_r-1\right)\Delta_r\Omega\right)\end{pmatrix}, \ \mathbf{e}_t(.) = \frac{1}{\sqrt{n_t}}\begin{pmatrix}1\\ \exp\left(-j2\pi\Delta_t\Omega\right)\\ \exp\left(-j2\pi 2\Delta_t\Omega\right)\\ .\\ .\\ .\\ \exp\left(-j2\pi\left(n_t-1\right)\Delta_t\Omega\right)\end{pmatrix}, \qquad (9)$$
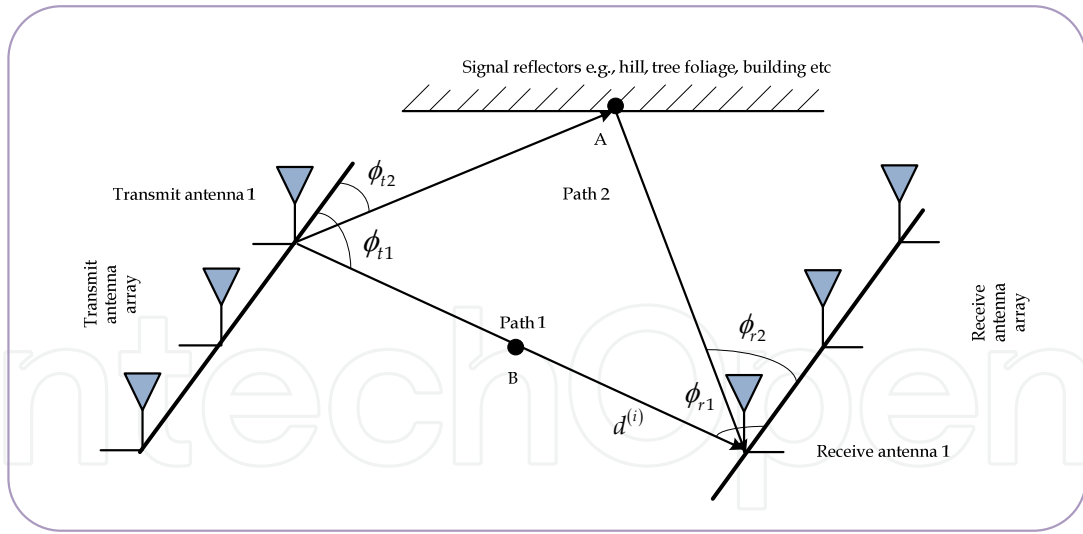
Figure 5. A MIMO channel with a direct path 1 and a reflected path 2. The channel is a concatenation of two channels H' and H'' with virtual relays A and B

From (9), the notation ϕ is the angle of incidence of the LOS onto the receive antenna array and a is the signal attenuation. In a reasonable sense, the condition that as long as

$$\Omega_{t1} \neq \Omega_{t2} \ \mathrm{mod} \ \frac{1}{\Delta_t} \ \text{and} \ \Omega_{r1} \neq \Omega_{r2} \ \mathrm{mod} \ \frac{1}{\Delta_r}$$

then the matrix $\mathbf{H}$ is of rank 2 holds. That is, the maximum number of independent rows or columns of the matrix is 2. Based on the defined condition, we let $\Delta_t = L_t \div n_t$ and $\Delta_r = L_r \div n_r$ whereby L_t and L_r are normalized lengths of transmit and receive arrays, respectively. As a subsequence, the implication is explained as follows. When the number of antennas in each HPN is increased for any fixed normalized length of arrays, the factor denoted by Δ will decrease and from the modulo operation, the directional cosine denoted by Ω will increase proportionately. This might cause ill-conditioned $\mathbf{H}$ with impossible inverse. To make $\mathbf{H}$ well-conditioned so that its inverse can be computed, the angular separations Ω_t and Ω_r should satisfy the following:

$$\Omega_t = \cos\phi_{t2} - \cos\phi_{t1}, \; L_t = n_t \Delta_t \; \text{ and } \; \Omega_r = \cos\phi_{r2} - \cos\phi_{r1}, \; L_r = n_r \Delta_r. \tag{10}$$

Moreover, in order to view the influence of multipath, $\mathbf{H}$ is re-written as $\mathbf{H} = \mathbf{H}''\mathbf{H}'$, where $\mathbf{H}'$ is a 2 by n_t matrix while $\mathbf{H}''$ is an n_r by 2 matrix. Consequently, the capacity limit of the channel with LOS and reflected paths in an HPN based mesh link is given as:

$$R_{LoS+\text{Re}\,flect} = \log_2\left(1 + SINR_j \times \|\mathbf{H}\|^2\right), \text{ bits / s / Hz}$$

$$R_{LoS+\text{Re}\,flect} = \log_2\left(1 + SINR_j \times \|\mathbf{H}''\mathbf{H}'\|^2\right), \text{ bits / s / Hz} \tag{11}$$

$$= \log_2\left(1 + SINR_j \times 2 \times \left(\left(a_1^b\right)^2 + 2a_1^b a_2^b + \left(a_2^b\right)^2\right)\right), \text{bits / s / Hz},$$

where

$$\left(a_1^b\right)^2 = a_1^2 n_t n_r, \left(a_2^b\right)^2 = a_2^2 n_t n_r,$$

Suppose fading channels are assumed, then the single link of IEEE 802.11n based HPNs can be characterized by stochastic channel behaviours. Statistical MIMO channel models are adopted to capture the key properties that enable spatial multiplexing (Tse & Viswanath, 2005). For instance, given an arbitrary number of physical paths between the transmitter and the receiver, the channel matrix $\mathbf{H}$ may be written as:

$$\mathbf{H} = \sum_i^{no\ of\ multipaths} a_i^b \mathbf{e}_r\left(\Omega_{ri}\right)\mathbf{e}_t\left(\Omega_{ti}\right)^*, \tag{12}$$

where a_i^b, $\mathbf{e}_r(\Omega)$ and $\mathbf{e}_t(\Omega)$ take the definition provided in (9). From (11) and without loss of generality, the capacity limit of the MIMO multipath fading channel can similarly be written as:

$$R_{multipath} = \log_2\left(1 + SINR_j \times \|\mathbf{H}\|^2\right), \text{ bits / s / Hz}$$

$$= \log_2\left(1 + SINR_j \times \left\|\sum_i^{multipaths} a_i^b \mathbf{e}_r\left(\Omega_{ri}\right)\mathbf{e}_t\left(\Omega_{ti}\right)^*\right\|^2\right), \text{ bits / s / Hz} \tag{13}$$

In conclusion, if the number of physical paths is two then the expression of capacity over multipath phenomenon (13) simply reduces to the expression (11) of the direct and reflected paths. Clearly from expression (13), one notes that increasing the multiplicity of paths of a single wireless link and the number of antennas at each HPN in (11) or (13) will increase the capacity limit of the wireless mesh links, depicted in (4) due to MIMO technology benefits.

4. Achievable capacity limit of HPNs in a mesh network

4.1. Practical considerations

In order to obtain the achievable capacity bound for the HPN (the dual channel dual radio) based mesh network we consider a typical static wireless mesh network. Suppose the network is assumed to consist of varying n number of HPNs upto 50 nodes with a fixed area of deployment region (i.e., 5 Km by 5 Km). Also to generalize our derivations and only apply specific cases later with numerical examples, we employ the approach presented by Kyasanur and Vaidya (2005) in order to investigate the impact of number of channels and interfaces on the capacity of multi-channel wireless networks. In our derivations, the term "channel" will refer to a part of frequency spectrum with some specified bandwidth and the term "radio" will mean the network interface card. Let us assume that the HPNs based mesh network has c channels and every node is equipped with m interfaces so that the relation between the number of interface cards and channels is $2 \leq m \leq c$. Each interface card can only transmit and receive data on any one channel at a given time, that is half-duplex communication. Thus, the mesh network of m interfaces per node, and c channels will be noted as (m, c)-network. Suppose each channel can support a fixed data rate of $R = R_{multipath}$, independent of number of non-overlapping channels of the network. Then, the total data rate possible by using all c non-overlapping channels is Rc. The number of non-overlapping channels can be increased by utilizing extra frequency spectrum of the standard technologies. For example, IEEE 802.11a standard technology uses 5 GHz band and has a capability of 24+ non-overlapping channels (c = 24+) each of 20 MHz bandwidth size (W = 20 MHz). Moreover, the IEEE 802.11n standard technology implements MIMO channels with bandwidth size of 40 MHz (Cisco systems, 2011).

4.2. Capacity limit for regular placement in real network

Consider Figure 6 that shows the topology of HPNs up to a maximum of 50 nodes placed regularly in a 5km by 5km of an area. This network scenario reflects a typical wireless mesh network set-ups in rural and remote areas where inter node distance is large and the land-scape affects network performance. It should be seen that the separation distance between the source and the destination HPNs are assumed to take the longest route with a mean line joining the two nodes computed to be 6505 m. The regular placement of nodes ensures that there are no any two HPNs that are placed within a radius less than 700 m. The main reason for this decision is to avoid interference between close neighbours. It will be discussed in detail how this placement criteria is ensured using the carrier sense multiple access with

collision avoidance (CSMA/CA) in IEEE 802.11 standards (IEEE 802.11 standard working group, 1999). In this topology setting, the regular placement of nodes on a fixed area will be termed as an arbitrary network. That is, the location of nodes and traffic patterns can be controlled as introduced by Gupta and Kumar (2000). Controlling nodes' placement locations and the traffic patterns makes the derived capacity bounds to be viewed as *the best case* capacity bounds with results remaining applicable to any network. As introduced by Gupta and Kumar, the aggregate *end to end* network throughput over a given flow or a set of flows is measured in terms of "bit-meters/sec". That is the network is said to transport one "bit-meter/sec" when one bit has been transported across a distance of one meter in one second.

Theorem 1: The E2E upper bound on capacity of a statically assigned channel network of type (m,c) -arbitrary regular placement of nodes when, $\dfrac{c}{m} = \mathrm{O}(n)$, is given as $\mathrm{O}\left(nR\sqrt{\dfrac{mc}{\delta}} \right)$, bit-meters/sec.

Proof: For the best case capacity limit, let's assume that multiple interfaces of HPNs receive and transmit on interference free channels. This assumption is reasonable with the HPNs that transmit directionally but receive and ensure connectivity omnidirectionally. As the number of channels is much larger than the number of interfaces. Thus, given that each HPN has a constant radio range, the spatial reuse is considered to be proportional to the physical area of the network. Let the node density δ be uniform with distribution regularity equals to one (i.e., probability equals to one) throught the deployment area.
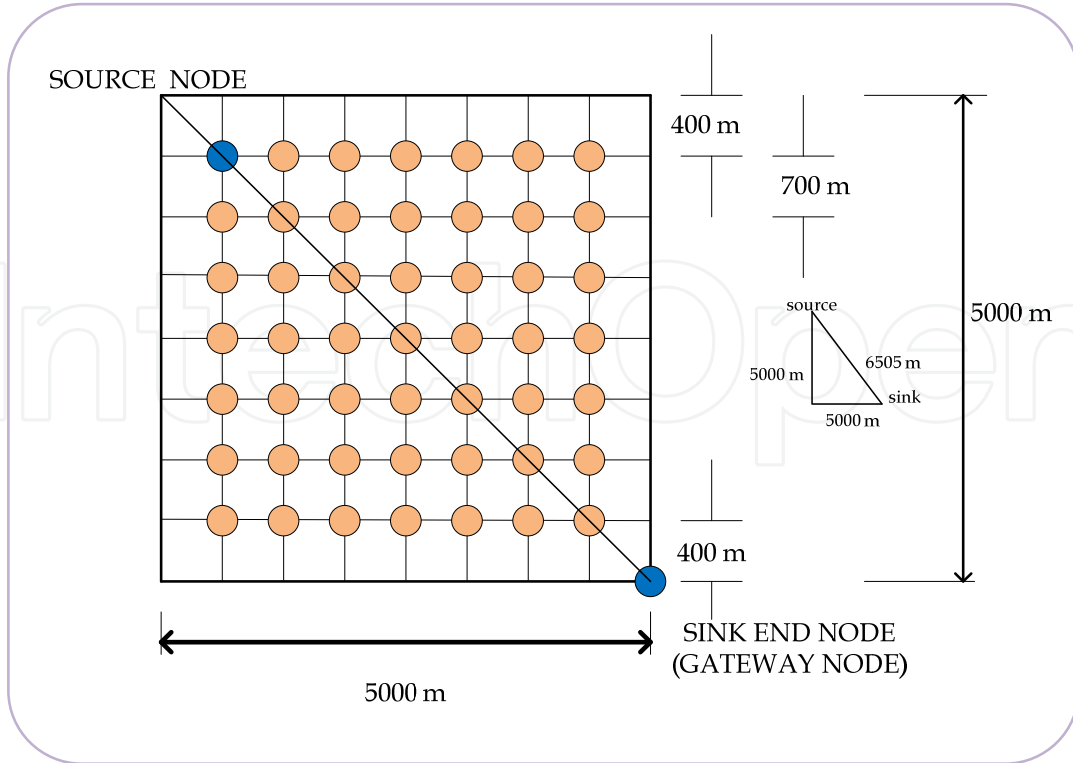
Figure 6. Regular placement of HPNs in a 5 km x 5 km

The physical area of deployment, A, can be related to the total number of HPNs by $A = \dfrac{n}{\delta}$. Consider also that, the capacity of each channel, R, is proportional to the physical area in accordance to the relation, $R = kA = k\dfrac{n}{\delta}$ for some constant k (in bits/s/square meters). Suppose each source HPN can generate packets from higher layers protocol at a rate of λ bits/sec and the mean seperation distance between the source and destination HPN pairs is $\overline{L}$ meters (via multiple hops), then the E2E network capacity of the network is (Gupta & Kumar, 2000):

$$\lambda n \overline{L}, \text{ bit} - \text{meters / sec} \qquad (14)$$

The expression in (14) is evaluated without taking into account the lower layer number of frequency channels, interference, path loss effects and number of interface cards. In addition, in order to relate this high level network capacity with actual number of hops in a multi-hop wireless network, the overall bits transported in the network can be evaluated as follows. Suppose bit b, $1 \leq b \leq \lambda n$ (bits/sec), traverses $h(b)$ hops on the path from its source to its destination, where the hth hop traverses a distance of r_b^h, then the overall bits transported in the network in every second is summed and is related to (14) as:

$$\lambda n \overline{L} \leq \sum_{b=1}^{\lambda n} \sum_{h=1}^{h(b)} r_b^h, \text{ bit} - \text{meters / sec} , \qquad (15)$$

The inequality in (15) holds since the mean length of the line joining the source and destination, is at most equal to the distance traversed by a bit from its sources to its destination (Kyasanur & Vaidya, 2005).

Let us define X to be the total number of hops traversed by all bits in a second, i.e., $X = \sum_{b=1}^{\lambda n} X(b)$. Therefore, the number of bits transmitted by all nodes in a second (including bits forwarded) is equal to X (bits/sec). Since each HPN node has m interfaces, and each interface transmits over a frequency channel of bandwidth W, with a data rate R possible per channel, the total bits per second that can be transmitted by all interfaces is at most $\dfrac{Rmn}{2}$ (transporting a bit across one hop requires two interfaces, one each at the transmitting and the receiving nodes). Consequently, the relation between a single channel single link rate, the number of interface cards creating single links, the number of nodes in the network and the total number of hops traversed by all bits in every second is given by,

$$X \leq \dfrac{Rmn}{2}, \text{bits / sec} \qquad (16)$$

It should be noted that under the interference protocol model (Gupta & Kumar, 2000), a transmission over a hop of length r in a path loss link is successful only if there can be no
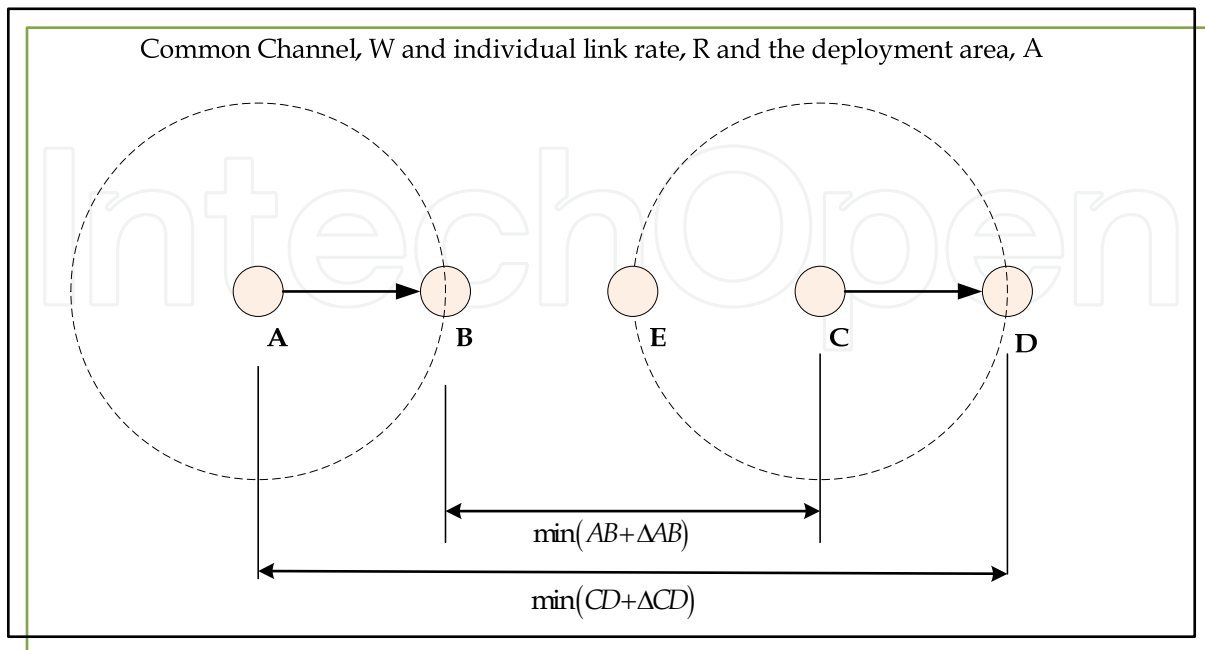
active transmitter within a distance of $(1 + \Delta)r$. In IEEE 802.11a/b/g/n standards the medium access control (MAC) layer protocols execute carrier sense multiple access with collision avoidance (CSMA/CA) mechanism that ensures that this condition is satisfied. Figure 7 illustrates this type of collision avoidance mechanism. To illustrate this concept further, suppose node A is transmitting a bit to node B, while node C is simultaneously transmitting a bit to node D and both sessions are over a common frequency channel, W. Then, using the interference protocol model and the geometry sufficient for successful reception, node E cannot transmit at the same time. Mathematically, one has

$$d(C,B) \geq (1+\Delta)d(A,B) \text{ and } d(A,D) \geq (1+\Delta)d(C,D) \tag{17}$$

Adding the two inequalities together, and applying the triangle inequality to (17), we can obtain the inequality in (18),

$$d(B,D) \geq \frac{\Delta}{2}\big(d(A,B) + d(C,D)\big) \tag{18}$$

Therefore, in collision avoidance (CSMA/CA) principle of IEEE standards , expression (18) can be viewed as each hop covering a disk of radius $\frac{\Delta}{2}$ times the length of the hop around each receiver. As shown by Figure 7, the total area covered by all hops must be bounded above by the total area of the deployment (domain, A). The seperation distance between receiver B and transmitter C is at least $(AB + \Delta AB)$ and that of transmitter A and receiver D is at least $(CD + \Delta CD)$.

Common Channel, W and individual link rate, R and the deployment area, A

A   B   E   C   D

min($AB + \Delta AB$)

min($CD + \Delta CD$)

Figure 7. Topology of HPNs and Geometry

From the geometry of Figure 7, we sum over all channels (which can potentially transport Rc bits per second) and obtain the constraint formulated as,

$$\sum_{b=1}^{\lambda n} \sum_{h=1}^{h(b)} \frac{\pi \Delta^2}{4} \left(r_b^h \right)^2 \leq ARc, \tag{19}$$

this can be rewritten as,

$$\sum_{b=1}^{\lambda n} \sum_{h=1}^{h(b)} \frac{1}{X} \left(r_b^h \right)^2 \leq \frac{4ARc}{\pi \Delta^2 X} \tag{20}$$

Since the expression on the left hand side in (20) is convex, one obtains,

$$\left(\sum_{b=1}^{\lambda n} \sum_{h=1}^{h(b)} \frac{1}{X} r_b^h \right)^2 \leq \sum_{b=1}^{\lambda n} \sum_{h=1}^{h(b)} \frac{1}{X} \left(r_b^h \right)^2 \tag{21}$$

Therefore, from (20) and (21) one gets,

$$\sum_{b=1}^{\lambda n} \sum_{h=1}^{h(b)} r_b^h \leq \sqrt{\frac{4ARcX}{\pi \Delta^2}} \tag{22}$$

Substituting for X from (16) in (22), and using expression (15) we have,

$$C_{mesh} \leq nR \sqrt{\frac{2mc}{\delta \pi \Delta^2}}, \text{ bit – meters / sec} \tag{23}$$

Therefore, the E2E asymptotically upper bound capacity limit for a scaling number nodes with node density δ, and static channel assignment without channel switching mechanisms in HPN network is given by

$$\begin{aligned} \lambda n \overline{L} &= O\left(nR \sqrt{\frac{mc}{\delta}} \right), \text{ bit – meters / sec } \textit{for varying node density} \\ \lambda n \overline{L} &= O\left(nR \sqrt{mc} \right), \text{ bit – meters / sec } \textit{for constant node density} \end{aligned} \tag{24}$$

4.3. Capacity limit for irregular placement in real network

Consider Figure 8 that shows the topology of HPNs up to a maximum of 50 nodes placed irregularly in a 5km by 5km of an area. This network scenario reflects typical wireless mesh network set-ups in rural and remote areas where inter node distance is large and the land-scape affects network performance. To avoid interference, it is assumed that no any two HPNs are placed within a radius less than 400 m at the edge and less than 700m toward the centre of the deployment area. However, between any two HPNs the largest separation

distance is allowed as much possible as the size of the area can accommodate. The diagram indicates one of the possible settlement distribution patterns of the Internet users in community based networks such as the case of Peebles valley mesh (PVM) networks.

Theorem 2: The E2E upper bound on capacity of a statically assigned channel network of type (m,c)-arbitrary irregular placement of nodes when, $\dfrac{c}{m} = \mathrm{O}(n)$, is given as,

$$\lambda n \overline{L} = O\left(Rn\sqrt{\dfrac{mc}{\delta p}} \right) \text{ bit-meters/sec.}$$
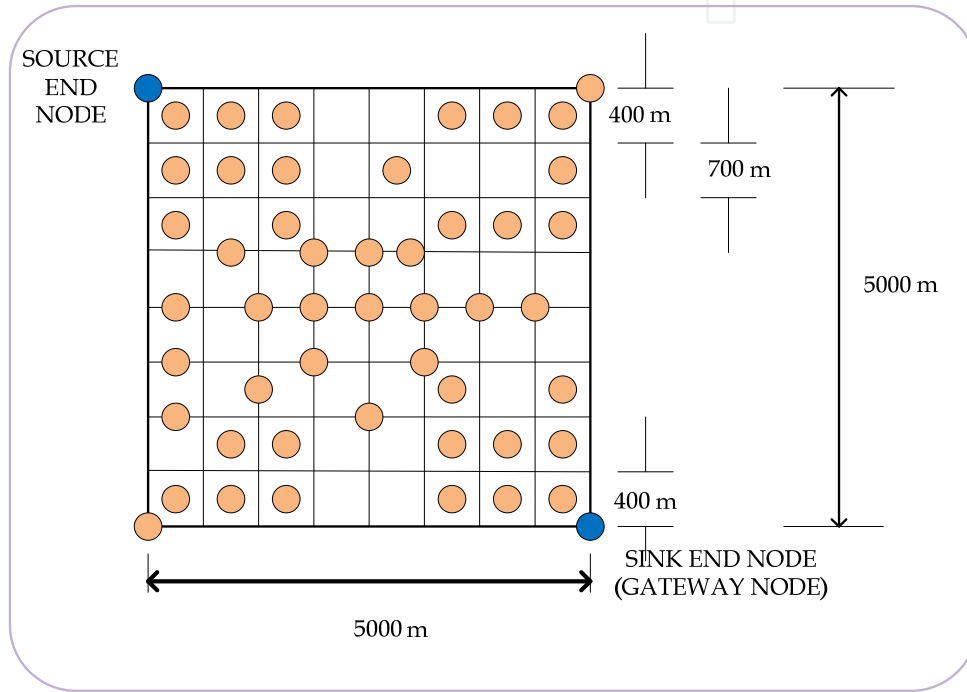
Figure 8. Irregular placement of HPNs in a 5 km x 5 km

Proof: Let us consider that in irregular static networks, the node density δ varies over space (i.e., an area) but stays constant at any given time since nodes are taken to be static. Suppose we let the node density δ to vary over space with irregularity rate (probability), $0 < p < 1$ then the area A is defined as $A = \dfrac{n}{\delta p}$. Therefore, capacity of the network will depend on the expected average node density, δp of an irregular placement as well as the number of nodes, n. Additionally, HPN nodes have m interfaces per node and with a data rate of R possible per channel. Then, the total bits per second that can be transmitted by all interfaces in the network and all channels is at most $\dfrac{Rnmc}{2}$.

If we let $X = \sum_{b=1}^{\lambda n} X(b)$ as the number of bits transmitted by all nodes in a second (including bits forwarded). From (22), we found out that

$$\sum_{b=1}^{hn}\sum_{h=1}^{h(b)} r_b^h \leq \sqrt{\frac{4ARRnmc}{2\pi\Delta^2}} \tag{25}$$

Alternatively, it has been established that

$$\sum_{b=1}^{hn}\sum_{h=1}^{h(b)} r_b^h = \lambda n\overline{L} \tag{26}$$

We have

$$\lambda n\overline{L} \leq R\sqrt{\frac{2Anmc}{\pi\Delta^2}} = Rn\sqrt{\frac{2mc}{\delta p\pi\Delta^2}}$$

$$\lambda n\overline{L} = O\left(Rn\sqrt{\frac{mc}{\delta p}}\right), \text{bit} - \text{meters} / \text{seconds} \tag{27}$$

## 4.4. Capacity limit for clustered placement in real network

Suppose that n nodes are arbitrarily located (a cluster fashion) on a square of a fixed area with LOS ensured between any two neighbouring nodes shown in Figure 9. Note that the deployment area is fixed to 5 km by 5 km. To avoid interference no two HPNs can be placed at a radius less than 400 m near the edge and less than 700 m toward the centre of the deployment area. Thus, within a cluster a minimum separation distance of 700 m is considered, while any largest separation distance possible is considered between clusters. Figure 9 shows the regularly clustered topology indicating how far as possible the separation distance between the source and destination HPNs. The diagram depicts typical rural community networks such as Peebles valley mesh (PVM) networks. The community mesh network is considered to adopt such a distribution pattern and the goal would be to find the achievable capacity over wireless mesh networks.

Theorem 3: The E2E upper bound on capacity of statically a signed channel network of type (m,c)-arbitrary clustered placement of nodes when $\frac{c}{m} = O(n)$ is given as

$\lambda n\overline{L} = O\left(R\sqrt{\frac{nmc}{1}\left(\frac{n_1}{\delta_1} + \frac{n_2}{\delta_2}\right)}\right)$ in bit-meters/sec, where R is the min (R_1, R_2), n_1 are number of

nodes in a regular cluster and n_2 are number of clusters in the network.

Proof: We assume *a clustered placement* of the mesh network as *a special case of the regular HPNs placement*. However, in this case the node densities are respectively, $\delta_1 = \frac{n_1}{A_1}$ as the density of nodes within a cluster consisting of n_1 nodes occupying A_1 geographical area and $\delta_2 = \frac{n_2}{A_2}$ as the density of clusters consisting of n_2 clusters occupying A_2 of an area. This

assumption is reasonable since HPNs within a cluster use a shorter transmission range compared to that range that is being used by nodes while communicating between clusters. The application layer generates the E2E capacity according to Gupta and Kumar model. This capacity depends on the number of nodes and can be simplified as $\lambda n \overline{L}$, bit-meters/sec.
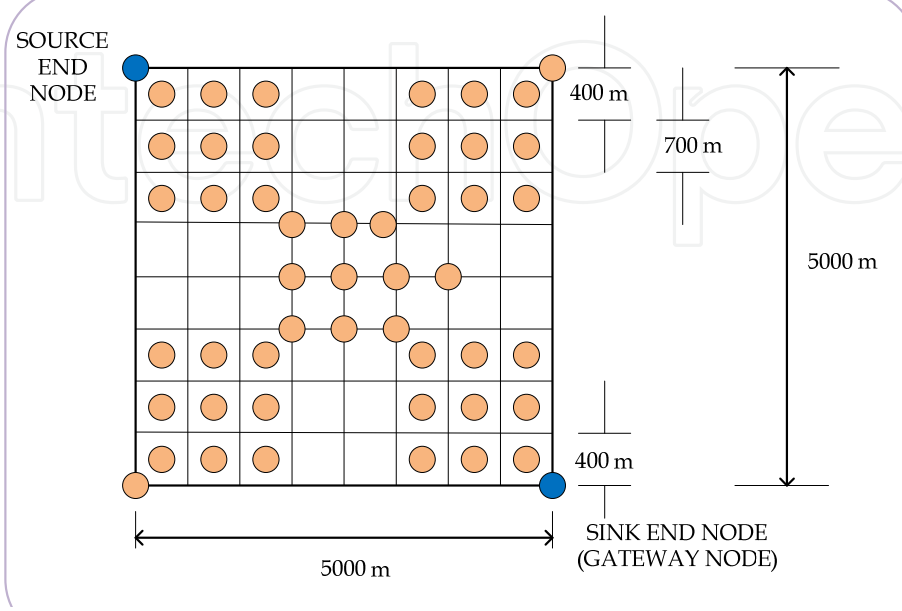
Figure 9. Regularly clustered placement of HPNs in a 5 km x 5 km

Suppose bit b, $1 \leq b \leq \lambda n$ (bits/sec), traverses $h(b)$ hops on the path from its source to its destination, where the h-th hop traverses a distance of $r_b^h = r_b^h(\delta_1) + r_b^h(\delta_2)$ (having intra-cluster and inter-cluster hop distances), then one obtains by summing over all bits in the network:

$$\lambda n \overline{L} \leq \sum_{b=1}^{\lambda n} \sum_{h=1}^{h(b)} r_b^h, \text{ bit} - \text{meters / sec} \tag{28}$$

Let us define X to be the total number of hops traversed by all bits in a second, i.e., $X = \sum_{b=1}^{\lambda n} X(b)$. Therefore, the number of bits transmitted by all nodes in a second (including bits forwarded) is equal to X (bits/sec). It is known that each HPN node has m interfaces, and each interface transmits over a frequency channel of bandwidth W, with a data rate R per channel, the total bits per second that can be transmitted by all interfaces is at most $\dfrac{Rmn}{2}$ (transporting a bit across one hop requires two interfaces, one each at the transmitting and the receiving nodes). But in clustered networks where bits traverse the intra cluster hops and inter cluster hops with R1 and R2 rates respectively. R takes the minimum rate since R drops with distance. Consequently, we have,

$$X \leq \frac{Rmn}{2}, \text{bits / sec} \tag{29}$$

Therefore, using similar arguments and steps provided in the *Proof of Theorem 1*, the interference constraint protocol of the clustered mesh network will still hold. The derived E2E capacity limit is then upper bound as

$$\lambda n\overline{L} \leq R\sqrt{\frac{2nmc}{\pi\Delta^2}\left(\frac{n_1}{\delta_1} + \frac{n_2}{\delta_2}\right)}, \text{ bit} - \text{meters} / \text{sec} \tag{30}$$

Hence, the asymptotic end to end upper bound capacity limit for a scaling number of nodes with node density δ_1 and cluster density δ_2, and statically assigned channels in HPN network is given by

$$\lambda n\overline{L} = \text{O}\left(R\sqrt{\frac{nmc}{1}\left(\frac{n_1}{\delta_1} + \frac{n_2}{\delta_2}\right)}\right), \text{ bit} - \text{meters} / \text{sec} \tag{31}$$

5. Numerical examples using the Peebles valley mesh

Tables 1 and 2 shows useful data that can be used to determine the achievable capacity limit over long links with direct LOS of about 6.505 km from one end of the network to the other. The data mimics the physical scenario of PVM as compared to the data sheet values of IEEE 802.11a and IEEE 802.11n air interfaces, respectively. The computed capacity values assume CSMA/CA and the protocol model whereby a transmission over one link is successful only if there is no active transmitter within a distance of $(1+\Delta)d$. That is, the distance d is the range between a transmitter and receiver, and Δ signifies a fraction of one hop distance needed to ensure collision-free transmission. The assumption of protocol model is reasonable in sparsely placed nodes in rural set-up whereby interference effects can be neglected without loss of generality. Furthermore, let the size of data carriers in OFDM scheme be, $M_c = 48$ with each HPN having an 8dBi omni-directional antenna and 20 dBi being the directional antenna (i.e., the combined antenna gain is 630.96 (6.3096 times 100) and α in a hilly and foliage area is taken approximately to be three between the frequency channels 5.15 GHz and 5.85 GHz (Durgin et al., 1998). Then, from the capacity limit expression in Section 3, practical data rates can be obtained.

5.1. Single link achievable capacity

Table 1, lists parameters needed to evaluate the achievable data rate for all wireless streams of a single link IEEE 802.11a radios. A comparison is made between the achievable data rate computed using data from the IEEE 802.11a air interface data-sheet and the data rate of the IEEE 802.11a air interface constructed from BB4all™ architecture. It is observed that while specifications of other parameters are kept the same in both cases, the combined antenna gain is taken to be 9 dBi from the data-sheet and that of BB4all™ architecture to be 28 dBi. With these antenna gains, the achievable data rate in standard architecture is 60.792 Mbps compared to 183.30 Mbps for the HPNs. This numerical result is explained as follows. When

transmission power is kept the same for both cases, an increase in antenna gain due to more focussed beams increases capacity substantially. Thus, the HPNs have capacity gains over the standard IEEE 802.11a devices.

Parameter	Data sheet	BB4all ™ architecture
Maximum single link range (metres), d	~6505	~6505
Modulation scheme	OFDM	OFDM
RF Industrial, Science & Medical (ISM) band (GHz), f	5	5
Number of spatial streams, L	2	2
Combined antenna gain (dBi), $K_{antenna}$	9	28
Channel width (MHz) of IEEE 802.11 a, W	20	20
Maximum output power (mWatts) of IEEE 802.11a radio, P	50	50
Reference distance (metres), d_0	5	5
AWGN (mWatts), N_0	1e-10	1e-10
Achievable data rate (Mbps) for all streams, R	60.792	183.30

Table 1. IEEE 802.11a air interface single link capacity

Table 2 lists parameters needed to evaluate the achievable data rate for all wireless streams of a single link IEEE 802.11n radios. A comparison is made between the achievable data rate computed using data from the IEEE 802.11n air interface data-sheet and the data from the BB4all™ architecture. It is observed that while specifications of other parameters are kept the same in both cases, the datasheet combined antenna gain is taken to be 7 dBi and that of BB4all™ architecture to be 28 dBi. With these antenna gains, the achievable data rate is 291.33 Mbps in standard architecture compared to 570 Mbps for the HPNs. This numerical result is explained as follows. When transmission power and the size of the MIMO are constant, an increase in antenna gain increases capacity substantially. Thus, the HPNs have capacity gains over the standard IEEE 802.11n devices.

Parameter	Data sheet	BB4all™ architecture
Maximum single link range (metres), d	~6505	~6505
Modulation scheme	OFDM	OFDM
RF Industrial, Science & Medical (ISM) band (GHz), f	5	5
Number of spatial streams (2xMIMO), L	2	2
Combined antenna gain (dBi), $K_{antenna}$	7	28
Channel width (MHz) of IEEE 802.11 a, W	40	40
Maximum output power (mWatts) of IEEE 802.11a radio, P	100	100
Reference distance (metres), d_0	5	5
AWGN (mWatts), N_0	1e-10	1e-10
Achievable data rate (Mbps) for all streams, R	291.33	570

Table 2. IEEE 802.11n air interface single link capacity

5.2. End to end achievable capacity under different HPN placements

Tables 3 and 4 show the E2E numerical values of capacity, right from the ethernet at one end of the network to ethernet at the other end of the network. Consider a wireless mesh network made up of IEEE 802.11a and IEEE 802.11n (Cisco systems, 2011) HPNs. Suppose typical information available are: the radio interfaces $m=2$, the orthogonal channel $c=2$, the deployment area $A = 5000\,m \times 5000\,m$ and the bandwidth $W=20\,Mhz$ and carrier frequency of 5.85 GHz. Assume that Carrier sense multiple access with collision avoidance (CSMA/CA) protocol is employed in order to identify pairs nodes that can simultaneously transmit (Kodialam and Nandagopal, 2005). In this protocol, neighbours of both an intended transmitter and receiver have to refrain from both transmission and reception in order to avoid collisions. Practically, we can let $\Delta =10\%$ of one hop distance to be sufficient enough to prevent neighbouring nodes from transmitting on the same subchannel at the same time. One hop distance is approximately 2100 m. This study also assumed an optimized link state routing (OLSR) protocol that proactively maintains fresh lists of destinations and their routes (Johnson, 2007). These routing tables are periodically distributed in the network. The protocol ensures that a route to a particular destination is immediately available. Couto et al (2005) proposed an expected transmission count (ETX) metric to calculate the expected number of retransmissions that are required for a packet to travel to and from a destination. ETX metric is adapted in this study as a default routing metric to determine the amount of successful packets at any receiver node from a transmitting neighbour within a window period. ETX metric is also viewed as a high-throughput path metric for multi-hop wireless mesh network (Couti et al., 2005). Using such information, we can illustrate the end to end

(E2E) capacity limit with practical examples of network deployments. In particular, consider the following cases:

a. Regular pattern when $n=10$ and when $n=50$, the node density is distributed with uniform probability of one.

b. Irregular pattern when $n=10$ and when $n=50$. Assume that the average distance of source-destination pair is 6505 m. The value enables the computation of achievable capacity over direct LOS path (i.e., without multi-hops) between the source and destination nodes. Nodes are assummed to be placed irregularly with a rate (probability) p, taken arbitrally as 0.9. Note that $0<p<1$. The choice of p depicts the severeness of the irregular placements of HPNs, with smaller values of p depicts more irregular environment and larger value shows that the placement of nodes in an area is carefully planned.

c. Regularly clustered pattern above when $n=10$ and 5 clusters each of 2 nodes, as well as when $n=50$ with 5 clusters each of 10 nodes.

HPNs placement in a 5 km x 5 km area	No. of HPNs	Achievable link capacity (Mbps)	E2E achievable capacity (Mbps)
Regular at p = 100%	10	R(2100 m) = 281.12	0.5192
	50	R(700 m) = 376.22	0.9322
Irregular at p = 90%	10	R(2100 m) = 281.12	0.5473
	50	R(700 m) = 376.22	0.9827
Clustered	10	R_1(700 m) = 376.22 R_2(4200 m)= 221.13 R = min (R_1, R_2)	0.4202
	50	R_1(700 m) = 376.22 R_2(1400 m)= 316.22 R = min (R_1, R_2)	0.5374

Table 3. IEEE 802.11a of HPNs of BB4all ™ architecture

HPNs placement in a 5 km x 5 km area	No. of HPNs	Achievable link capacity (Mbps)	E2E achievable capacity (Mbps)
Regular at p = 100%	10	R(2100 m) = 722.24	1.3339
	50	R(700 m) = 912.44	2.2609
Irregular at p = 90%	10	R(2100 m) = 722.24	1.4061
	50	R(700 m) = 912.44	2.3832
Clustered	10	R_1(700 m) = 912.44 R_2(4200 m)= 602.24 R = min (R_1, R_2)	1.1443
	50	R_1(700 m) = 912.44 R_2(1400 m)= 792.44 R = min (R_1, R_2)	2.0201

Table 4. IEEE 802.11n of HPNs of BB4all™ architecture

Table 5 illustrates the achievable E2E capacity results of the BB4allTM architecture compared to closely related work on dual radio dual channel analytical results by Kyasanur and Vaidya (2005).

Dual-radio dual-channel mesh network	Consists of IEEE 802.11a HPNs: regularly placed	Consists of IEEE 802.11n HPNs: regularly placed	Arbitrary network of dual radio dual channel (Kyasanur and Vaidya, 2005)
Upper bound capacity value (of 50 nodes) in Mbps in a 5 km x 5 km	0.9322	2.2609	0.01

Table 5. E2E achievable capacity gain of BB4all™ architecture

5.3. Discussions on E2E achievable capacity

It should be noted from both Tables 3 and 4 that in a fixed area of 5 km by 5 km, the E2E achievable capacity evaluated shows that there is lower capacity when number of HPNs is ten than when the number is 50 in all node placement scenarios. The main reason is that a series of long links created between any two immediate nodes degrades the achievable E2E capacity. This was proven by single link capacity models in Section 3. For instance, at ten HPNs in the fixed sized network, the hop distances are much larger than the case for 50 HPNs. In each hop, the propagating signal faces path loss effects due to terrain irregularity, foliage and wireless medium conductivity. The implication is that signal traversing longer hop distances are faced with higher attenuation and lower E2E capacity than signal propa-

gating over shorter hops. The numerical results plotted in the tables 3 and 4 also showed that HPNs distributed with irregularity rate (probability) of 90% provides the highest E2E achievable capacity limit compared to the three node placement scenarios. This means that when HPNs are distributed with irregularity rate of 90%, the probability of finding some nodes in some areas will likely reduce by 10%. However, with the same number of nodes and fixed area of deployment, the inter hop distances where nodes occur will be much smaller by 10% than in regular placements. But shorter hops imply higher capacity if and only if there is no interference as we have noted with single links. Moreover, according to Li et al. (2001), increasing or keeping constant the number of nodes placed in a fixed area automatically increases or keeps constant the average node density. The average node density is inversely proportional to the E2E capacity according to *Theorem 2*. Thus, a lower average density in an irregular node placement for the same number of nodes will yield a higher E2E capacity if and only if the area of deployment is fixed or decreased. Using similar argument, when values of p is decreased (i.e., 0.8, 0.7, 0.6, etc), the average δ decreases proportionately and if the area of deployment is fixed or reduced then for the same number of nodes, the capacity will increase. Interestingly, Tables 3 and 4 showed that in regularly clustered placements, the E2E capacity limit values are least compared to other placement scenarios. The explanation is motivated by viewing that there is long distances between clusters and shorter distances between HPNs within a cluster. While, the former situation exacerbates achievable capacity, the latter improves capacity. The contributing factor within a cluster is then the inter-cluster distances that degrades the overall capacity that can be achieved.

At n = 50 the achievable E2E capacity for clustered placement is almost two times less than one related to regular or irregular patterns in the case of IEEE 802.11a air interface network, but in the case of IEEE 802.11n air interface network it becomes more or less comparable. In Section 3, characterization of influence of multipath, multiple antennas, and hop distance on the link capacity revealed that multipath and distance predominantly affect capacity in IEEE 802.11a air interface, while multipath and the number of antennas predominantly influence the achievable capacity in IEEE 802.11n air interface. Because clustered placements irrespective of the number of antennas per HPN provide longer hop distances between one cluster and other, one expects much worse E2E capacity value in a clustered IEEE 802.11a air interface compared to regular and irregular placements.

It was also noted that network throughput dropped significantly from source HPN to the destination HPN or gateway. In particular, the drop was by about 99% across 3 long distance hops and by about 99% across 3 long distance hops considering regularly deployed HPNs from Tables 3 and 4, respectively. The general explanation is that, the channel gain drops with increase in propagation distance, and there are also overhead losses associated with medium access control (MAC) and the multi-hop routing such that the number of packets sent is not equal to the number of packets received successfully. Despite this observation, HPNs derived from IEEE 802.11n radios have a better E2E capacity achievable mainly due to the MIMO technologies that are capable of combating multi-path fading (Franceschetti et al., 2009).

In arbitral network, with a combined antenna gain of 9dBi, hop distance of 700 m, bandwidth of 20 MHz, transmitted power output of 100 mWatts and 1e-10 Watts, the

conventional analytical results of Kyasanur and Vaidya (2005) was compared with the HPNs of the BB4all™ architecture. Data from Table 5 shows that HPNs of the latter with special radios and antenna arrangements is more superior to the HPNs with standard antenna gains. While all cases considered dual radio dual channel specifications, the HPNs of the BB4all™ architecture have higher throughput antenna configurations than the work proposed by Kyasanur and Vaidya (2005).

6. Conclusion and future work

The BB4all™ architecture makes use of omni-directional antennas to maintain mesh connectivity, while directional antennas support information relay over long distances with high power gains. It was found that the impact of multipath and MIMO of IEEE 802.11a/n air interfaces on achievable capacity can be characterized by OFDM modulation scheme, antenna configurations, and multiple streaming of frames or packets. Both the analytical and numerical results showed that the higher the dimensions of these parameters, the higher the achievable capacity due to benefits derived from channel diversity. It was also confirmed based on related previous works that increasing the number of interfaces per HPN and channels in the network does increase the achievable E2E capacity in any arbitral network placement. One of the contribution of this study was the innovation constructed to improve performance of the commercially available WLAN devices. The pillar of innovation was that increasing the antenna gains could improve capacity of real networks even without increasing the power settings of the transmitter.

The CSIR Meraka Institute, South Africa, through living lab initiatives, are currently gathering field data regarding end-to-end capacity that is experienced by rural community Internet users. The findings will be assessed with a view of considering possible improvements of future network architectures that can provide high data rates. Other possible exploration of increasing capacity of community networks (i.e., Peebles valley mesh in South Africa) include utilization of unused frequency (TV white space) spectrum. The TV white spaces spectrum fosters high capacity signal transmissions over long distances in rural terrains. Thus, cognitive and foraging radio techniques are promising tools toward spectrum and energy efficient network management for the next billion internet users. It should also be noted that, although the theoretical derivations were applied to the PVM network, they could also be applied to other rural deployments as well.

Author details

Thomas Olwal, Moshe Masonta, Fisseha Mekuria and Kobus Roux
CSIR Meraka Institute, South Africa

Acknowledgement

7. References

Abhayawardhana, V.S.; Wassell, I. J.; Crosby, D.; Sellars, M. P. & Brown, M. G., (2004). Comparison of empirical propagation path loss models for fixed wireless access systems, *In Vehicular Technology Conference,* 2005. ISSN: 1550-2252.

BelAir Networks. (2006). Capacity of wireless mesh networks: understanding single radio, dual radio and multi-radio wireless mesh networks, *White paper*, pp. 1-16, BDMC00040-C02.

Berthilson, L. & Pascual, A. E. (2007). Link performance parameters in IEEE 802.11: How to increase the throughput of a wireless long distance link, *White paper*, April 2007.

Bracewell, R. N. (1986). *The Fourier transform and its applications*, McGraw Hill, 1986.

Cisco Systems Inc. (2011). *Channels and maximum power settings for Cisco Aironet lightweight access points*. Pp. 1-130, No: OL-11321-08.

Couto, D. S. J. D.; Aguayo, D; Bicket, J. & Morris, R. (2005). A high-throughput path metric for multi-hop wireless routing. *Wireless Networks Journal*, Vol. 11, No. 4, pp. 419-434.

Durgin, G.; Rappaport, T. S. & Xu, H. (1998). Measurements and models for radio path loss and penetration loss in and around homes and trees at 5.85 GHz. *IEEE Transactions on Communications,* Vol. 46, No. 11, pp. 1484-1496.

Eriksson, J.; Agarwal, S.; Bahl, P. & Padhye, J. (2006). Feasibility study of mesh networks for all-wireless offices, In Proceedings of MobiSys'06, June 19-22, 2006, Sweden, pp. 69-82: ISBN: 1-59593-195-3.

Franceschetti, M,; Migliore, M. D. & Minero, P. (2009). The capacity of wireless networks: information-theoretic and physical limits. *IEEE Trans. on Information Theory*. Vol. 55. No. 8, pp. 3413-3424.

Gupta, P., and Kumar, P. R. (2000). The capacity of wireless networks. *IEEE Transactions on 4 Information Theory*, Vol. 46, no. 2, pp. 388-404, March 2000: ISSN: 0018-9448.

Intini, A. L. (2000). OFDM wireless networks: Standard IEEE 802.11a. *Technical report at the University of California Santa Barbara.*

Ishmael, J., Bury, S., Pezaros, D., and Race, N. (2008). Deployment rural community wireless mesh networks. IEEE Internet Computing. Vol. (2): 22-29: DOI: 1089-7801/08/2008 IEEE.

IEEE 802.11 Standard Working Group, (1999). Wireless LAN medium access control (MAC) and physical layer specifications: high speed physical layer in the 5 GHz band, IEEE 802.11a standard.

Johnson, D. (2007). Evaluation of a single radio rural mesh network in South Africa, *Proceedings of International Conference on Information and Communication Technologies*, Bangalore, India, December 2007, ISBN:

Johnson, D. & Roux, K. (2008). Building rural wireless networks: lesions learnt and future directions, *Proceedings of 2008 ACM Workshop on Wireless Networks and Systems for Developing Regions*, San Francisco, California, USA, 19 September 2008, pp. 17- 22, ISBN: 978-1-60558-190-3

Kobus, R., et al. (2009). Broadband for all (BB4all)™: CSIR Science Scope, Magazine, Magazine, Vol. 3, no. 3, January 2009, pp. 16-17.

Kodialam, M., and Nandagopal. T. (2005). Characterizing the capacity region in multi-radio multi-channel wireless mesh networks. *MobiCom'05*, August 28-September 2, 2005, Cologne, Germany: ISBN: 1-59593-020-5.

Kyasanur, P. & Vaidya, N. H. (2004). Routing and interface assignment in multi-channel multi-interface wireless networks, *Technical Report of Department of computer science at the University of Illinois at Urban-Champaign*, pp. 1-7, ANI-0125859.

Kyasanur, P. & Vaidya, N. H. (2005). Capacity of multi-channel wireless networks: impact of number of channels and interfaces, *Technical Report of Department of computer science at the University of Illinois at Urban-Champaign*, March 2, 2005.

Li, J.; Blake, C.; De Couto, D. S. J.; Lee, H. I. & Morris, R. (2001). Capacity of Ad hoc Wireless Networks, *Proceedings of MobiCom Conference*, July 2001, Rome, Italy, pp. 61-69, ISBN: 1-58113-486-X

Mesh Dynamics Inc., (2010). Wireless mesh networks that scale like switch stacks, Available at *http://www.meshdynamics.com*.

Makitla, I. ; Makan, A. & Roux, K. (2010). Broadband provision to underprivileged rural communities. *In Proceedings of CSIR 3rd Biennial Conference 2010*. Also available at www.csir.co.za : Reference no: HE04-PO-F.

Mekuria, F.; Masonta, M. T., and Olwal, T.O. (2012). Future networks to enable wireless broadband technologies and services for the next billion users, *In Proceeding Future Network & Mobile Summit 2012*, Berlin, Germany, 4-6 July 2012.

Miu, A., Balakrishnan, H., and Koksal, C. E. (2007). Multi-radio diversity in wireless networks, *Wireless Networks*, pp.13:779-798. DOI:10.1007/s11276-006-9854-2.

Olwal, T. O. (2010). *Decentralised dynamic power control for wireless backbone mesh networks*, PhD Thesis, University of Paris-EST and Tshwane University of Technology.

Olwal, T. O et al. (2011). Optimal control of transmission power management in wireless backbone mesh networks, In: *Wireless Mesh Networks*, Funabiki, N (Eds). PP. 3-28, InTech, ISBN: 978-953-307-519-8, Croatia.

Tse, D., and Viswanath, P. (2005). *Fundamentals of wireless communication*, Chapter 5 and Chapter 7, University of California Berkley.